



## Effect of anode area on the sensing mechanism of vertical GaN Schottky barrier diode temperature sensor

Ji-Yao Du(都继瑶), Xiao-Bo Li(李小波), Tao-Fei Pu(蒲涛飞), and Jin-Ping Ao(敖金平)

**Citation:** Chin. Phys. B, 2022, 31 (4): 047701. DOI: 10.1088/1674-1056/ac3223

Journal homepage: <http://cpb.iphy.ac.cn>; <http://iopscience.iop.org/cpb>

**What follows is a list of articles you may be interested in**

## Strain-modulated ultrafast magneto-optic dynamics of graphene nanoflakes decorated with transition-metal atoms

Yiming Zhang(张一鸣), Jing Liu(刘景), Chun Li(李春), Wei Jin(金蔚), Georgios Lefkidis, and Wolfgang Hübner

Chin. Phys. B, 2021, 30 (9): 097702. DOI: 10.1088/1674-1056/abef1

## Band alignment between $\text{NiO}_x$ and nonpolar/semipolar GaN planes for selective-area-doped termination structure

Ji-Yao Du(都继瑶), Ji-Yu Zhou(周继禹), Xiao-Bo Li(李小波), Tao-Fei Pu(蒲涛飞), Liu-An Li(李柳暗), Xin-Zhi Liu(刘新智), and Jin-Ping Ao(敖金平)

Chin. Phys. B, 2021, 30 (6): 067701. DOI: 10.1088/1674-1056/abdb21

## Monolithic epitaxy and optoelectronic properties of single-crystalline $\gamma\text{-In}_2\text{Se}_3$ thin films on mica

Xibo Yin(尹锡波), Yifan Shen(沈逸凡), Chaofan Xu(徐超凡), Jing He(贺靖), Junye Li(李俊烨), Haining Ji(姬海宁), Jianwei Wang(王建伟), Handong Li(李含冬), Xiaohong Zhu(朱小红), Xiaobin Niu(牛晓滨), and Zhiming Wang(王志明)

Chin. Phys. B, 2021, 30 (1): 017701. DOI: 10.1088/1674-1056/abcf32

## Recent advances, perspectives, and challenges inferroelectric synapses

Bo-Bo Tian(田博博), Ni Zhong(钟妮), Chun-Gang Duan(段纯刚)

Chin. Phys. B, 2020, 29 (9): 097701. DOI: 10.1088/1674-1056/aba603

## First-principles calculation of influences of La-doping on electronic structures of KNN lead-free ceramics

Ting Wang(王挺), Yan-Chen Fan(樊晏辰), Jie Xing(邢洁), Ze Xu(徐泽), Geng Li(李庚), Ke Wang(王轲), Jia-Gang Wu(吴家刚), Jian-Guo Zhu(朱建国)

Chin. Phys. B, 2020, 29 (6): 067702. DOI: 10.1088/1674-1056/ab84db

# Effect of anode area on the sensing mechanism of vertical GaN Schottky barrier diode temperature sensor

Ji-Yao Du(都继瑶)<sup>1</sup>, Xiao-Bo Li(李小波)<sup>2</sup>, Tao-Fei Pu(蒲涛飞)<sup>2,†</sup>, and Jin-Ping Ao(敖金平)<sup>2</sup>

<sup>1</sup>School of Automation and Electrical Engineering, Shenyang Ligong University, Shenyang 110159, China

<sup>2</sup>Institute of Technology and Science, Tokushima University, Tokushima, Japan

(Received 3 June 2021; revised manuscript received 14 October 2021; accepted manuscript online 22 October 2021)

Effect of anode area on temperature sensing ability is investigated for a vertical GaN Schottky-barrier-diode sensor. The current-voltage-temperature characteristics are comparable to each other for Schottky barrier diodes with different anode areas, excepting the series resistance. In the sub-threshold region, the contribution of series resistance on the sensitivity can be ignored due to the relatively small current. The sensitivity is dominated by the current density. A large anode area is helpful for enhancing the sensitivity at the same current level. In the fully turn-on region, the contribution of series resistance dominates the sensitivity. Unfortunately, a large series resistance degrades the temperature error and linearity, implying that a larger anode area will help to decrease the series resistance and to improve the sensing ability.

**Keywords:** GaN, temperature sensor, Schottky contact, vertical diode

**PACS:** 77.84.Bw, 73.40.Kp, 52.59.Mv, 82.80.Pv

**DOI:** 10.1088/1674-1056/ac3223

## 1. Introduction

Gallium nitride (GaN) based Schottky barrier diodes (SBDs) are key components for the next-generation high power and high switching frequency devices, which are commonly adopted in switching power supply, wireless communications, drivers, and so on.<sup>[1–4]</sup> Compared with the planar SBDs fabricated on the AlGaN/GaN structure, vertical devices can achieve high power density and high breakdown voltage by simply increasing the drift layer thickness other than extending the gate-to-drain distance.<sup>[5–10]</sup> Therefore, vertical devices are preferable to sink chip size and decrease the cost. Especially, with the tremendous progress in high quality GaN substrates, vertical GaN SBDs have attracted a great deal of attention in recent years.

On the other hand, GaN devices commonly generate heat during static on-state and on/off switching.<sup>[11]</sup> This heat dissipation will drastically increase the junction temperature especially for vertical devices which handle higher power densities. Generally, electrical parameters of SBDs are temperature-dependent and will be degraded under a relatively high temperature.<sup>[12]</sup> Hence, temperature monitoring plays a key role in ensuring safe operation or quality control. However, the accuracy and reliability of the conventional thermocouples or resistive temperature sensors do not meet the request of high temperature environment.

Alternatively, GaN based Schottky barrier diodes (SBDs) are a kind of promising candidates for *in situ* temperature sensor applications due to the wide bandgap, good linearity, and long-term stability. In our previous study, lateral, quasi-vertical and vertical GaN-compatible temperature sen-

sors were fabricated and evaluated with thermally stable TiN anode.<sup>[13–16]</sup> When the SBD works in sub-threshold region, the forward voltage at a fixed relatively small current level decreases linearly versus temperature. It was demonstrated that the sensitivity of the lateral and quasi-vertical SBD is dependent on the anode area. However, the effect of anode area of a vertical diode on the sensing characteristics is not investigated extensively. In this work, vertical GaN SBDs with various anode sizes are proposed to investigate the effect of anode area. It is found that a large anode area helps to decrease the series resistance and to enhance the sensitivity. The current density and series resistance dominate the sensitivity in sub-threshold region and fully turn-on region, respectively.

## 2. Experiments and characterization

The vertical GaN SBDs (Fig. 1) were fabricated on a commercial free-standing wafer. The epitaxial structure and the main processes were similar with our previous work.<sup>[15]</sup> The electrode material and the sputtering conditions are listed in Fig. 1. To improve the high temperature interface reliability, we adopted a thermally stable TiN as the anode electrode. Compared with the Ni and NiN anodes in our previous work,<sup>[14–17]</sup> the work function of TiN is approximately 4.7 eV. The relatively small Schottky barrier height (SBH,  $\Phi_b \sim 0.6$  eV) is beneficial to decrease the turn-on voltage ( $V_{on}$ ) and on-state power loss.<sup>[17]</sup> On the other hand, the TiN can effectively suppress the interface reaction between GaN and the conventional metal anode. Good Schottky contact properties are maintained even after the 800 °C annealing for several minutes.<sup>[18]</sup> Those results demonstrate that TiN is promis-

<sup>†</sup>Corresponding author. E-mail: fbc.ptf@126.com

ing for GaN SBD temperature sensor applications. Herein, we focus on evaluating the effect of anode area on the sensitivity. A series of SBDs with different anode radii ( $R = 55 \mu\text{m}$ ,  $70 \mu\text{m}$ , and  $85 \mu\text{m}$ ) were fabricated. To investigate the temperature sensing ability and the mechanism, current-voltage-temperature ( $I$ - $V$ - $T$ ) characteristics were measured from  $25^\circ\text{C}$  to  $200^\circ\text{C}$  with steps of  $25^\circ\text{C}$ .

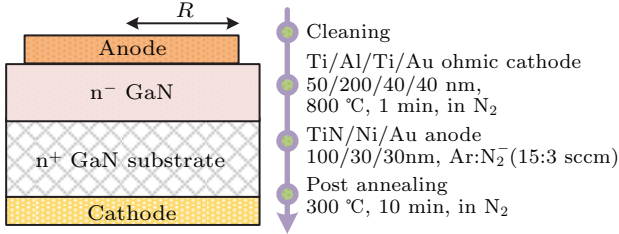


**Fig. 1.** Schematic view of the vertical GaN SBD temperature sensors with different anode radii ( $R$ ). The corresponding main fabrication processes are also listed.

### 3. Results and discussions

The typical  $I$ - $V$ - $T$  characteristics of SBD with an anode radius of  $55 \mu\text{m}$  were recorded, as shown in Fig. 2(a). The  $V_{\text{on}}$  extracted by linear fitting the forward region is about  $0.47 \text{ V}$ , which is consistent with previous reports.<sup>[14,17]</sup> In addition, the  $I$ - $V$ - $T$  curves show a zero-temperature coefficient (ZTC) point. Obviously, the variation of current versus temperature are different in the bias regions above and below the ZTC point (approximately  $0.6 \text{ V}$ ). For the small forward voltage ( $V_F$ ) region (below ZTC point), the voltage at a specific current value decreases gradually with the increasing temperature (negative coefficient). Noticeably, above the ZTC point (relatively high  $V_F$  region), the voltage at a specific current value increases gradually with the increasing temperature (positive coefficient).

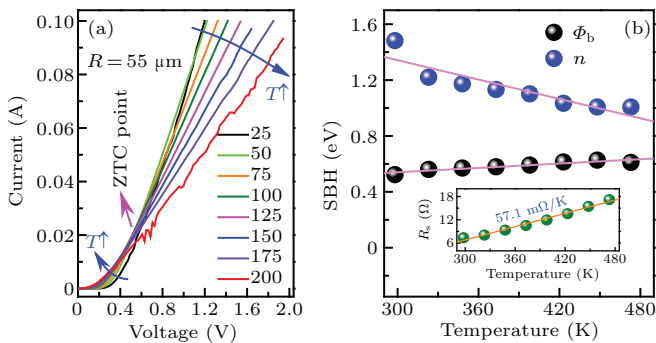


**Fig. 2.** The  $I$ - $V$ - $T$  characteristics (a) of vertical GaN SBD with an anode radius of  $55 \mu\text{m}$ . (b) The relationship between key parameters and temperature.

Theoretically, the  $I$ - $V$ - $T$  curves of the SBD follow the thermal emission (thermionic emission, TE) model. The forward current  $I_D$  under  $V_F > 3kT/q$  reads<sup>[17]</sup>

$$I_D = A_e A^* T^2 \exp\left(-\frac{q\Phi_b}{kT}\right) \exp\left(\frac{q(V_F - I_D R_s)}{nkT}\right). \quad (1)$$

The  $V_F$  is then solved as

$$V_F = n\Phi_b + \frac{nkT}{q} \left[ \ln\left(\frac{I_D}{A_e A^*}\right) - 2\ln(T) \right] + I_D R_s, \quad (2)$$

where  $A_e$ ,  $T$ ,  $q$ ,  $n$ ,  $k$ ,  $A^*$  and  $R_s$  are the Schottky anode area, Kelvin temperature, electronic charge, ideality factor, Boltzmann constant, Richardson constant ( $26.9 \text{ A}\cdot\text{cm}^{-2}\cdot\text{K}^{-2}$  in our calculation) and series resistance, respectively. Based on Eq. (2), the key parameters ( $\Phi_b$ ,  $n$ , and  $R_s$ ) of the SBD versus temperature with an anode radius of  $55 \mu\text{m}$  are fitted and plotted in Fig. 2(b). It is demonstrated that the  $\Phi_b$  increases from  $0.52 \text{ eV}$  to  $0.62 \text{ eV}$  linearly with the increasing  $T$ , while the  $n$  decreases from  $1.4$  to  $1.0$  linearly. In addition, we also find that the  $R_s$  increases from  $7.3 \Omega$  to  $17.2 \Omega$  with temperature in a slope of  $57.1 \text{ m}\Omega/\text{K}$ . The variation of  $\Phi_b$  and  $n$  versus temperature are not consistent with the TE model, in which those values should be constants. The possible reason is attributed to the spatial fluctuation of  $\Phi_b$  at interface, namely, the barrier height inhomogeneous effect.<sup>[19]</sup> The carrier at relatively high temperature gains more energy and then overcomes the high barrier patch, resulting in a high average barrier height.

To evaluate the effect of anode radius on the electrical properties, the  $I$ - $V$ - $T$  characteristics of SBDs with anode radii of  $70 \mu\text{m}$  and  $85 \mu\text{m}$  are shown in Figs. 3(a) and 4(a), respectively. The  $I$ - $V$ - $T$  characteristics of both diodes are comparable with that of the small anode one, except the forward voltage that reaches the compliance current. By fitting the  $I$ - $V$ - $T$  curves, the  $\Phi_b$  of the  $70 \mu\text{m}$  SBD increases from  $0.61 \text{ eV}$  to  $0.67 \text{ eV}$ , while the  $n$  decreases from  $1.2$  to  $1.0$  linearly with the increasing  $T$  (Fig. 3(b)). The  $\Phi_b$  of the  $85 \mu\text{m}$  SBD increases from  $0.56 \text{ eV}$  to  $0.67 \text{ eV}$ , while the  $n$  decreases from  $1.2$  to  $1.0$  linearly with the increasing  $T$  (Fig. 4(b)). Those values and the variation trends are comparable to each other, implying that other factors are the root causes. It is worth noting that the slopes of  $R_s$  are  $37.1 \text{ m}\Omega/\text{K}$  and  $26.3 \text{ m}\Omega/\text{K}$  for the  $70 \mu\text{m}$  (inset of Fig. 3(b)) and  $85 \mu\text{m}$  (inset of Fig. 4(b)) diodes, respectively. This indicates that the  $R_s$  presents an obvious effect at the voltage region above the ZTC point.

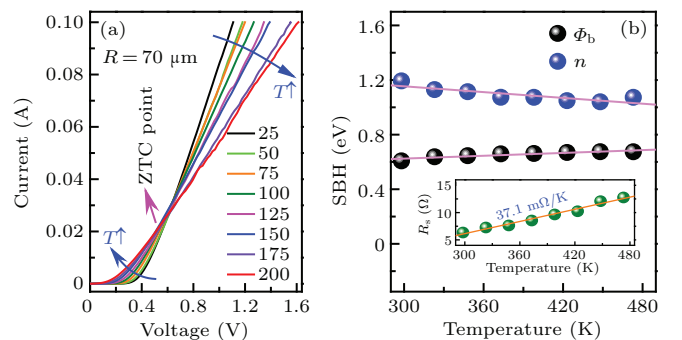


**Fig. 3.** The  $I$ - $V$ - $T$  characteristics (a) of the vertical GaN SBD with an anode radius of  $70 \mu\text{m}$ . (b) Relationship between key parameters and temperature.

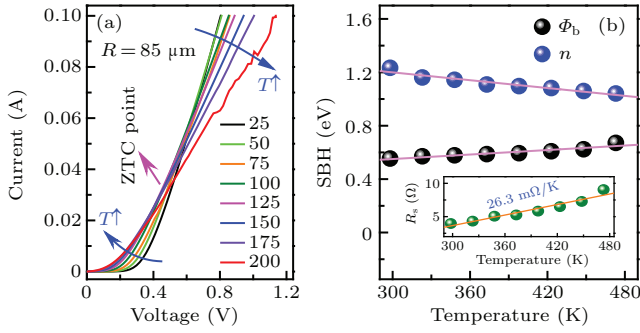


**Fig. 4.** The  $I$ - $V$ - $T$  characteristics (a) of the vertical GaN SBD with an anode radius of 85  $\mu\text{m}$ . (b) Relationship between key parameters and temperature.

The relationship between forward voltage and temperature is commonly used for determining the sensitivity. Furthermore, the sub-threshold region is preferable for temperature sensing application due to the relatively small power loss. When we choose a specific current ( $1 \times 10^{-5}$ ,  $1 \times 10^{-4}$ ,  $5 \times 10^{-4}$ , or  $1 \times 10^{-3}$  A in our experiment), the corresponding forward voltage on the  $I$ - $V$ - $T$  curves shifts negatively with the increasing temperature (Fig. 5(a)). The variation of this forward voltage versus temperature is then plotted in Fig. 5(b). Under four selected current levels, the corresponding forward voltage decreases with increasing temperatures, implying that the slope is negative (Fig. 5(b)). Based on the absolute slope of the fitting line, the measured sensitivities  $S_m$  are deduced to be 1.19, 1.2, 1.14, and 1.13 mV/K at  $1 \times 10^{-5}$ ,  $1 \times 10^{-4}$ ,  $5 \times 10^{-4}$ , and  $1 \times 10^{-3}$  A, respectively. Based on Eq. (2), the  $V_F$  is determined by three main parts. Firstly, we confirm that the production  $n\Phi_b$  shows slight dependence on temperature (Fig. 6(a)), which is ascribed to the opposite variation trends of  $\Phi_b$  and  $n$ . Secondly, the voltage drop contributed by the  $R_s$  ( $I \times dR_s/dT$ ) is smaller than 0.05 mV/K due to the small current in sub-threshold region. In addition, the non-linear part of  $\ln T$  can also be ignored in relatively small temperature range.<sup>[20]</sup> Hence, the sensitivity  $dV_F/dT$  is correlated with the current density  $I_D/A_e$  as

$$\frac{dV_F}{dT} \propto \frac{nK}{q} \ln \left( \frac{I_D}{A_e A^*} \right). \quad (3)$$

Therefore, the sensitivity is mainly determined by the ideality factor  $n$ , current level  $I_D$  and anode area  $A_e$ , but is not related with the wafer structure and diode geometry (circular, finger, dot, etc.). The above discussion is confirmed by the decreasing trend of sensitivity versus current level, which is proportional to the logarithms of current density (Fig. 6(b)). Because an ideal SBD follows the TE model, the change of anode material (variation in  $\Phi_b$  and reverse leakage current) has no direct effect on the sensitivity. In addition, although the interface reaction for the metal anode on GaN generates a relatively higher  $n$  and contributes to the sensitivity, the degradation of reliability is unsuitable for high temperature applications.

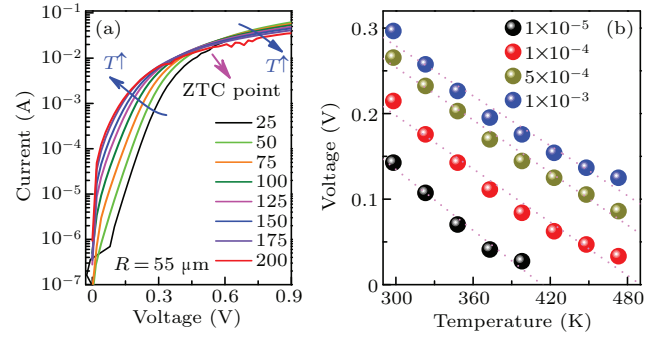


**Fig. 5.** (a) The sub-threshold region  $I$ - $V$ - $T$  characteristics of the vertical GaN SBD with an anode radius of 55  $\mu\text{m}$ . (b) The  $V_F$ - $T$  relationship at different current levels.

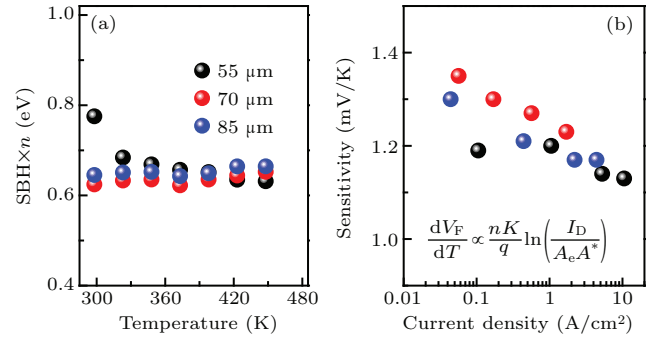


**Fig. 6.** (a) The production of SBH and  $n$  versus temperature. (b) The relationship between sensitivities and current density.

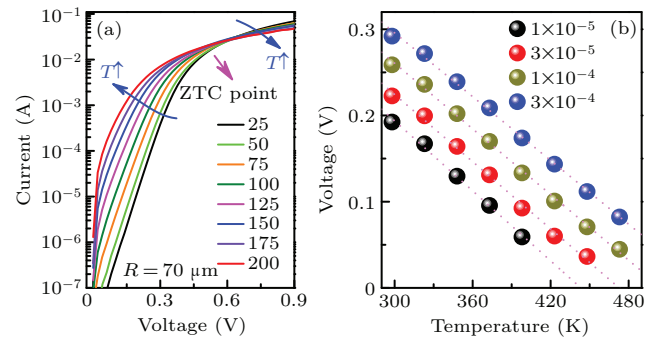


**Fig. 7.** (a) The sub-threshold region  $I$ - $V$ - $T$  characteristics of the vertical GaN SBD with an anode radius of 70  $\mu\text{m}$ . (b) The  $V_F$ - $T$  relationship at different current levels.

To evaluate the effect of anode area on the sensitivity, the sub-threshold region of  $I$ - $V$ - $T$  characteristics for the SBDs with anode radii of 70  $\mu\text{m}$  and 85  $\mu\text{m}$  are also plotted in Figs. 7(a) and 8(a), respectively. Then, the corresponding  $V_F$ - $T$  relationships at different currents with the fitting line are plotted in Figs. 7(b) and 8(b), respectively. Obviously, good linearity can be observed for all the  $V_F$ - $T$  curves, and the deduced sensitivities are summarized in Fig. 6(b). On the one hand, the production of  $\Phi_b$  and  $n$  shows slight dependence on temperature (Fig. 6(a)). On the other hand, the voltage drop contributed by the  $R_s$  ( $S_R$ , the production of  $dR_s/dT$  and current) is smaller than 0.04 mV/K. Therefore, the sensitivity is also proportional to the logarithms of current density (Fig. 6(b)). Therefore, when the sensor works at a specific current (sub-threshold region), a relatively larger anode area helps

to realize a smaller current density and to obtain a higher sensitivity.

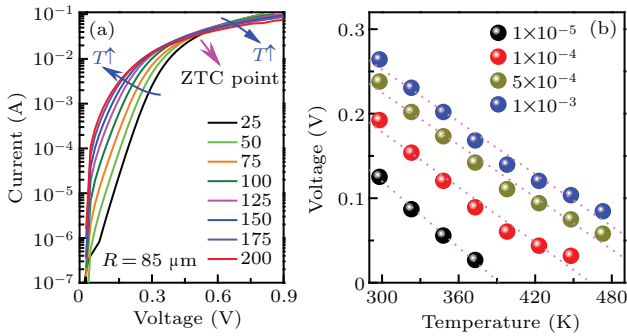


**Fig. 8.** (a) The sub-threshold region  $I$ - $V$ - $T$  characteristics of the vertical GaN SBD with an anode radius of 85  $\mu\text{m}$ . (b) The  $V_F$ - $T$  relationship at different current levels.

Unlike the sub-threshold region, the voltages at a specific current increase with the increasing temperature in the fully turn-on region, showing a positive slope above the ZTC point (Fig. 9(a)). At a current of 80 mA, the  $S_m$  values are deduced to be 3.81 mV/K, 2.04 mV/K, and 1.46 mV/K for the SBD with anode radii of 55  $\mu\text{m}$ , 70  $\mu\text{m}$ , and 85  $\mu\text{m}$ , respectively. However, the  $S_R$  values contributed by the  $R_s$  are calculated to be 4.56 mV/K, 2.97 mV/K, and 2.1 mV/K (Fig. 9(b)). Therefore, the  $S_m$  is dominated by the  $S_R$  in this region. We realize that the series resistance degrades the temperature error and linearity,<sup>[13]</sup> implying the fully turn-on region is not suitable for temperature sensor application. It is worth noting that a larger anode area helps to decrease the  $R_s$  and to improve the sensing ability.

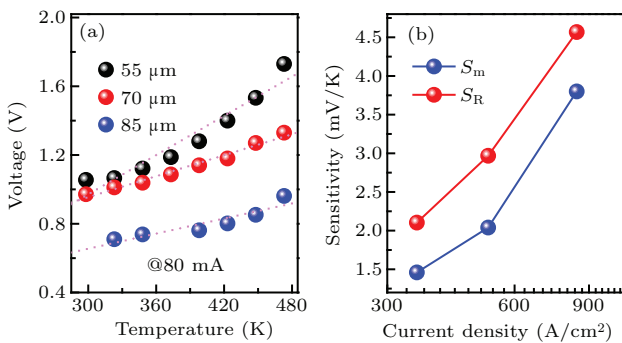


**Fig. 9.** (a) The  $V_F$ - $T$  relationship in fully turn-on region for the SBD with different anode radii. (b) The relationship between sensitivities and current density.

#### 4. Conclusions

In summary, we have fabricated vertical GaN SBD temperature sensors using a thermally stable TiN anode. Based on the  $I$ - $V$ - $T$  characteristics, the effect of anode area on the sensitivity is investigated. It is demonstrated that the  $I$ - $V$ - $T$  characteristics are comparable to each other for the diode with different anode areas, presenting a ZTC point and a typical

barrier inhomogeneous behavior. In addition, the  $R_s$  increases with temperature in slopes of 57.1 m $\Omega$ /K, 37.1 m $\Omega$ /K, and 26.3 m $\Omega$ /K for 50  $\mu\text{m}$ , 70  $\mu\text{m}$ , and 85  $\mu\text{m}$  diodes, respectively. When the voltage is below the ZTC bias point (sub-threshold range), the forward voltage decreases linearly versus temperature with a negative slope. The sensitivity deduced from the absolute value of slope is dominated by the current density, which follows the TE model. A large anode area helps to enhance the sensitivity at the same current level. When the voltage higher than the ZTC point (fully turn-on range), the forward voltage increases linearly with temperature in a positive slope. Then, the contribution of series resistance dominates the sensitivity. Under this condition, a larger anode area helps to decrease the series resistance and to improve the sensing ability.

#### Acknowledgements

The author Ji-Yao Du thanks Professor Hongwei Gao, the Dean of School of Automation and Electrical Engineering, for providing the post-doctoral position and the corporation opportunity with Tokushima University.

This work was supported by the Scientific Research Support Foundation for Introduced High-Level Talents of Shenyang Ligong University (Grant No. 1010147000914) and the Science and Technology Program of Ningbo (Grant No. 2019B10129).

#### References

- [1] Tsou C W, Wei K P, Lian Y W *et al.* 2015 *IEEE Electron Device Lett.* **37** 70
- [2] Bahat-Treidel E, Hilt O, Zhytnytska R *et al.* 2012 *IEEE Electron Device Lett.* **33** 357
- [3] Chang T F, Huang C F, Yang T Y *et al.* 2015 *Solid State Electron.* **105** 12
- [4] Dang K, Zhang J, Zhou H *et al.* 2019 *IEEE Trans. Ind. Electron.* **67** 6597
- [5] Saitoh Y, Sumiyoshi K, Okada M *et al.* 2010 *Appl. Phys. Exp.* **3** 081001
- [6] Tanaka N, Hasegawa K, Yasunishi K *et al.* 2015 *Appl. Phys. Exp.* **8** 071001
- [7] Han S, Yang S, Sheng K 2018 *IEEE Electron Device Lett.* **39** 572
- [8] Yang T H, Fu H, Fu K *et al.* 2020 *IEEE J. Electron Devices Soc.* **8** 857
- [9] Liu Z, Wang J, Gu H *et al.* 2019 *AIP Adv.* **9** 055016
- [10] Ren B, Liao M, Sumiya M *et al.* 2017 *Appl. Phys. Exp.* **10** 051001
- [11] Tsurumi N, Ueno H, Murata T *et al.* 2010 *IEEE Trans. Electron Devices* **57** 980
- [12] Zhou Y, Wang D, Ahyi C *et al.* 2007 *J. Appl. Phys.* **101** 024506
- [13] Li X, Pu T, Li X *et al.* 2020 *IEEE Trans. Electron Devices* **67** 1171
- [14] Li L, Chen J, Gu X *et al.* 2018 *Superlattices Microstruct.* **123** 274
- [15] Liu D P, Li X B, Pu T F *et al.* 2021 *Chin. Phys. B* **30** 038101
- [16] Wang Y, Pu T, Li X *et al.* 2021 *Mater. Sci. Semicond. Proc.* **125** 105628
- [17] Li L, Kishi A, Liu Q *et al.* 2014 *IEEE J. Electron Devices Soc.* **2** 168
- [18] Li L, Kishi A, Shiraishi T *et al.* 2013 *Jpn. J. Appl. Phys.* **52** 11
- [19] Yildirim N, Ejderha K and Turut A 2010 *J. Appl. Phys.* **108** 114506
- [20] Rao S, Pangallo G, Pezzimenti F *et al.* 2015 *IEEE Electron Device Lett.* **36** 720